



Urban air quality changes resulting from the lockdown period due to the COVID-19 pandemic

D. Galán-Madruga¹

Received: 13 February 2021 / Revised: 8 March 2022 / Accepted: 5 August 2022 / Published online: 20 August 2022

© The Author(s) under exclusive licence to Iranian Society of Environmentalists (IRSEN) and Science and Research Branch, Islamic Azad University 2022

Abstract

This work aims to quantify potential pollution level changes in an urban environment (Madrid city, Spain) located in South Europe due to the lockdown measures for preventing the SARS-CoV-2 transmission. Polluting 11 species commonly monitored in urban zones were attended. Except for O₃, a prompt target pollutant levels abatement was reached, intensely when implanted stricter measures and moderately along those measures' relaxing period. In the case of TH and CH₄, it is evidenced a progressive diminution over the lockdown period. While the highest decreasing average changes relapsed on NO_x (NO₂: –40.0% and NO: –33.3%) and VOCs (C₇H₈: –36.3% and C₆H₆: –32.8%), followed by SO₂ (–27.0%), PM₁₀ (–19.7%), CO (–16.6%), CH₄ (–14.7%), TH (–11.6%) and PM_{2,5} (–10.1%), the O₃ level slightly raised 0.4%. These changes were consistently dependent on the measurement station location, emphasizing urban background zones for SO₂, CO, C₆H₆, C₇H₈, TH and CH₄, suburban zones for PM_{2,5} and O₃, urban traffic sites for NO and PM₁₀, and keeping variations reasonably similar at all the stations in the case of NO₂. Those pollution changes were not translated in variations on geospatial pattern, except for NO, O₃ and SO₂. Although the researched urban atmosphere improvement was not attributable to meteorological conditions' variations, it was in line with the decline in traffic intensity. The evidenced outcomes might offer valuable clues to air quality managers in urban environments regarding decision-making in favor of applying punctual severe measures for quickly and considerably relieving polluting high load occurred in urban environments.

Keywords Air quality · COVID-19 pandemic · Geospatial analysis · Restrictive measures · Urban environment

Introduction

At the worldwide level, the major environmental risk to human health leads to atmospheric pollution. Recent studies sustain links between air pollutant exposure and harmful

effects on human beings (Miller and Newby 2019; Zhang et al. 2019). World Health Organization (WHO) reported 4.2 million deaths every year due to exposure to ambient air pollution (<http://www.who.int/airpollution/en/>, accessed August 11, 2020).

In this environmental frame, a new coronavirus (Severe Acute Respiratory Syndrome Corona Virus 2, SARS-CoV-2) appeared in December 2019 in Wuhan, Hubei province (China) (Bigdeli et al. 2021). This novel agent is the seventh coronavirus known to affect humans (Andersen et al. 2020) and causes an infectious disease known as COVID-19. On December 31, 2019, Chinese authorities reported the new coronavirus to the WHO (<https://www.who.int/news-room/detail/27-04-2020-who-timeline---covid-19>, last access August 12, 2020). The coronavirus disease COVID-19 manifests a human to human transmissibility (Rastogi et al. 2020). As a consequence of its rapid spread at the global level (Bherwani et al. 2021), the WHO declared the novel coronavirus outbreak a global pandemic on March 11, 2020 (WHO 2020a). Globally, the total number of confirmed

Editorial responsibility: Samareh Mirkia.

Core ideas Average decreases (range: –10 and –40%) were exhibited, except for O₃ (rise +0.4%). Distinct pollution changes in the whole target area, dependent on the zones. A standard pattern concerning urban air pollution changes was not globally sustained. Polluting changes resulted in geospatial NO, O₃ and SO₂ variations. Pollution drop was related to traffic restraints, not with meteorological variations.

✉ D. Galán-Madruga
david.galan@isciii.es

¹ Department of Atmospheric Pollution, National Center for Environment Health, Health Institute Carlos III, Ctra. Majadahonda a Pozuelo Km 2,2. Majadahonda, 28220 Madrid, Spain



cases exceeded 79 million and over 1.7 million deaths till December 27, 2020 (WHO 2020b).

Within this global context, in order to break the transmission string of the coronavirus disease 2019 in Spain, the Spanish authorities declared the state of alarm on March 14, 2020 (RD 463/2020), which included the limitation of the freedom of movement of people, suspension of the "in situ" educational activity in all centers and educative stages, containment measures of cultural facilities, recreational establishments and activities, among other. On March 29, 2020, the Spanish government imposed severer measures, aims at confinement (RD-ley 10/2020), suspending nonessential activities such as industrial and construction sectors up to April 13, 2020 and then returning to activity applying the initial restriction measures. The lockdown period's de-escalation process initiated on May 4, 2020, gradually aborting the restrictive measures. Thus, both mobility and commercial activities progressively expanded until June 21, 2020 (end date of the state of alarm (RD-ley 10/2020)). In order to offer to potential readers information concerning industrial activity before the lockdown period, in terms of pollutant emissions, the last reports published by Madrid Municipality can be visited in the next link: (i) https://www.madrid.es/UnidadesDescentralizadas/Sostenibilidad/EspeInf/EnergiayCC/04CambioClimatico/4aInventario/Ficheros/EmissionsInv2018_acc.pdf, accessed September 20, 2021 and, (ii) https://www.madrid.es/UnidadesDescentralizadas/Sostenibilidad/EspeInf/EnergiayCC/04CambioClimatico/4aInventario/Ficheros/GHGemissions2018_acc.pdf, accessed September 20, 2021.

Given that the scientific evidence points to the urban atmospheres as those most polluted (Raffy et al. 2017), as a consequence of the air pollutant release coming from numerous emission sources, the guiding thread of the present work is to quantify the impact of the lockdown measures on air quality, particularly to an urban zone. This temporal circumstance offers an unprecedented opportunity in order to provide valuable clues to urban air quality management, based on the application of restrictive temporal measures, which acquires the utmost importance in terms of elucidating whether the outcome could be applied on a global or local urban level, as well as evaluating whether those measures are common to the city set or, conversely, it is necessary to differ per zones within target urban environment.

While many countries enforced similar controlling measures, researchers commenced surveying potential air quality

changes derived from implementing those measures. In this sense, while several researchers studied the effect of COVID-19 lockdown on air quality in urban zones (Faridi et al. 2020; Li et al. 2020), the air pollutants' behavior in those areas still needs to be addressed. This one could result specifically for a concrete city and a particular lockdown period due to several factors. On the one hand, the diversity and levels of the air pollutants found in urban environments might differ among cities. Their release and occurrence into the urban atmosphere depend on both emission sources and the meteorological variables specifics to each zone. Similarly, the urban topographic profile might sum another differential factor as the lockdown period's duration.

For advancing in this subject, this work aims to quantify the impact of the strict measures enforced for controlling the COVID-19 spread on air quality in an important urban area of South Europe (Madrid city, Spain). For reaching this objective, they were addressed the next steps to (i) estimate the target air pollutant concentrations during the lockdown phase, (ii) compare current vs estimated polluting compound levels along the quarantine period, (iii) discern possible geo-spatial differences in the target pollutants' pattern within the researched surface during lockdown phase and (iv) elucidate the influence of emission sources and meteorological variables on potential air quality changes.

It was attended a wide range of air pollutants in order to develop the proposed aim, highlighting sulfur dioxide (SO₂), carbon monoxide (CO), nitrogen monoxide (NO), nitrogen dioxide (NO₂), airborne particulate matter (PM_{2.5} and PM₁₀), ozone (O₃), toluene (C₇H₈), benzene (C₆H₆), total hydrocarbons (TH) and methane (CH₄). As of now, several of those pollutants (TH and CH₄) are novel compounds within the scope discharged at the scientific level.

In order to expand the valuable knowledge reported by other authors which assessed the impact of the COVID-19 pandemic on urban air quality, this research is the first work conducted in an urban environment whose outcomes are explained in relied on the entire investigated domain and the monitored fixe zone, either urban traffic site and suburban emplacement or background location, respectively. Therefore, this work pretends to clarify whether the shutdown measures applied to the target urban environment are translated in common air quality changes within the whole city or differ per zones, which might attend as a scientific base for designing future air quality management strategies.



Materials and methods

Area of study and air quality dataset

In order to develop the previously mentioned objective, a case study was conducted in Madrid City (Community of Madrid, Spain). It is located in the center of the Iberian Peninsula and divided into 21 districts and 128 neighborhoods.

It is Spain's capital and the Spanish city with the highest population (over 3,000,000 inhabitants, National Statistical Institute 2019, <http://www.ine.es>). It has a surface of approximately 600 km² and an altitude of 650 m (above sea level). Therefore, population density data in Madrid City expressed as people per sq. km of land area is highly higher than those reached in the 27 Union European Member States (110, see <https://ec.europa.eu/eurostat/web/products-eurostat-news/-/DDN-20200430-1>, accessed November 26, 2020) and in the Community of Madrid (> 800, <https://www.comunidad.madrid/>, accessed November 26, 2020).

At the meteorological level, Madrid City is characterized by temperate winters and dry and warm summers. It is ranked as Csa according to the Köppen-Geiger climate classification (Kottek et al. 2006), with annual 2019 mean meteorological values of 16°C (−2 and 35°C, minimum and maximum, respectively), 0.8 l/m² (0 and 43.8 l/m²), 52% (3 and 99%), 944 mb (678 and 961 mb), 203 W/m² (8 and 381 W/m²) and 1.42 m/s (0.09 and 6.04 m/s) for temperature, rainfall, relative humidity, barometric pressure, solar radiation and wind speed, respectively.

As a piece of relevant atmospheric pollution information, 2019 annual polluting averages recorded by different fixed monitoring stations ranged between 5 and 12, 13 and 22, 9 and 12, 16 and 53, 0.3 and 0.7, 35 and 63 µg/m³, respectively, for SO₂, PM₁₀, PM_{2.5}, NO₂, CO and O₃, as 0.2 and 0.5 mg/m³ for CO (http://www.mambiente.munimadrid.es/opencms/export/sites/default/calibre/Anexos/Memoria_2019.pdf, accessed December 8, 2020).

The reference air quality dataset used in developing this work was acquired from Madrid City's open data portal (<http://www.mambiente.munimadrid.es>). The local administration assesses the urban air quality using an air quality monitoring network (AQMN). The network consists of fixed monitoring stations distributed within its territories. Although 24 fixed monitoring stations constitute Madrid city's AQMN, the studied domain involved those stations located in neighborhoods with a population density higher

than 50 inhabitants per hectares (see Fig. S1). The stations were organized based on two criteria: (i) location (urban or suburban) and (ii) main pollution source (traffic or background).

AQMN is managed by the municipal government, which assures the measured data validation and network maintenance. This data package comprises current air pollutant concentrations encompassing pollution data from January 2018 to August 2020. Information about all fixed stations is shown in Table S1 and Fig. S2. Measurement methods for monitoring target air pollutants are showed in Table S2.

Estimate of target air pollutant levels

To gauge potential air quality changes in the researched urban atmosphere, assessed polluting compounds' monthly average levels are estimated during the shutdown period based on each target pollutant's air quality trend.

At the scientific level, the simple linear regression-based analysis applied to time series is commonly used to estimate the target parameter's unknown values. Time series data streams are analyzed for knowing the underlying pattern of the data along the selected time. The time series analysis drives to build a fitting line between the dependent variable and independent ones (Barman and Choudhury 2020); therefore, it can be respected this quantitative estimating approach because predicting the time series' future values in function of its historical behavior.

A sub-dataset involving from January 2018 to February 2020 is considered for setting air quality trends in order to estimate target air pollutants' levels during the lockdown period (March–June 2020). To this end, it is developed the following sequence:

1. The time variable is converted to a numeric value on a scale of 1–26. Thus, numeric value 1 is assigned to January 2018 and so on until the last month (February 2020).
2. The stationarity index is calculated based on the relationship between the concentration averaged from similar months (example: all January months included in the sub-dataset) and the mean of all concentrations recorded in the sub-dataset.

3. The current monthly average concentration is adjusted concerning the stationarity index by dividing the current value by this parameter.
4. The time series trend is established applying a simple linear regression analysis between the adjusted current monthly average concentration (dependent variable) and the numeric value assigned to the time variable (independent one).
5. The adjusted current monthly average level is re-calculated based on the investigated times series trend.
6. The stationarity index adjustment on the re-calculated monthly average concentration is removed by multiplying both terms, thereby reaching the estimated average concentration value.

A relevant aspect within an estimation process leads to knowledge of its validity and confidence degree. For this reason, for testing the executed estimation analysis, monthly average concentrations during July and August 2020 were estimated according to the previously mentioned sequence and compared to current average monthly concentrations recorded by Madrid city's air quality monitoring network during those two months (estimated levels were considered as a dependent variable and current levels as independent one).

Then, both datasets (estimated and current levels over July and August 2020) were dissected by general linear regression considering the following metrics: (i) measure of the correlation between both items, (ii) statistical significance of the simple linear regression with one-way ANOVA, (iii) statistical significance of the regression coefficient of the independent variable and (iv) statistical significance between paired samples.

Geospatial analysis

Isoline maps were generated in order to discern potential changes in spatial distribution gradient across investigated surface concerning the target air pollutants and meteorological conditions. It is used the Surfer software for Windows (Win32): Surface Mapping System, v.6.04. (Golden Software, Inc., Golden, CO, USA) for building the isoline maps.

The kriging method, as a geostatistical estimation tool, applied on air quality measurements monitored at fixed stations let extrapolating the air pollutant concentrations and

meteorological variable values in those points were not measured (Beauchamp et al. 2018).

Emission sources and meteorological variables

Broadly, the emission sources are responsible for releasing pollutants into the atmosphere, while that meteorological conditions can affect their stability and dilution in the ambient air. Therefore, the combination of potential polluting focuses and meteorological features modulates pollutants' presence in the air. For this reason, both variables are susceptible to be studied within the exposed objective.

Concerning the emission sources, while numerous polluting focuses are found in urban environments (such as transport networks, industrial activities, commercial and residential), vehicular emissions are the main contributors to ambient air pollution in cities (Mayer 1999), which has been contrasted at the global level (Karagulian et al. 2015; Marinello et al. 2020). In the case study (Madrid city), road transport is responsible for 51, 61, 55 and 55% of the NO_x, PM₁₀, PM_{2.5} and CO emissions, respectively (MITECO 2019). Based on this evidence, they were studied monthly average traffic intensity data encompassed between January 2018 and June 2020 in order to link whether a possible change in the circulating vehicle number during the lockdown period would influence target urban air quality.

For similar reasons, it was addressed monthly meteorological data from January to June 2019 and 2020, respectively, such as wind speed and direction, temperature, relative humidity, pressure, solar radiation and rainfall to elucidate whether possible changes in those variables pattern results in target urban air quality changes over the quarantine period. It is necessary to indicate that meteorological data for 2018 is not available in Madrid's Municipality's open data portal.

To achieve this end, it was acquired data of traffic intensity and meteorological features from Madrid City's open data portal. A total of 59 permanent control points for recording traffic intensity and 23 stations for monitoring meteorological variables in the target domain were attended (see Table S3 and S4, respectively).

Finally, it is conducted a combined PCA-MLR (principal component analysis- multiple linear regression) analysis for testing whether the pattern jointed of road traffic and meteorological conditions was dissimilar in 2019 and 2020, which could explain target urban air quality changes. In this



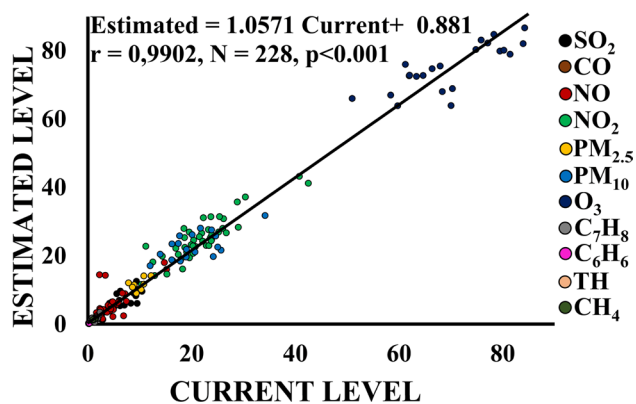


Fig. 1 Estimated vs current air pollutant levels (July and August 2020). Note: Units expressed in $\mu\text{g}/\text{m}^3$ except for CO in mg/m^3 .

sense, PCA is a classic chemometric technique applying a rotational algorithm to rate an original dataset of possibly correlated variables into a smaller set of values of linearly uncorrelated variables (Chen et al. 2019). The resulting sub-dataset keeps most of the original dataset's information (Li et al. 2019a, b). PCA technique used the varimax method and chose an eigenvalue > 1 (the Kaiser Criterion) as criteria

to select the principal components (PCs), which explained most of the cumulative variance. Subsequent PCs were accounted for until reaching up cumulative variance > 85%. Then, an MLR analysis was applied the outcomes obtained by the PCA process for quantifying the load of each selected variable within the PCs. It was used the previously enunciated variables' monthly average data from March to June to develop this approach, contrasting the outcomes reached in 2019 and 2020, given that 2018 meteorological data was not available.

Statistical analysis

Analysis of the dataset was performed using IBM SPSS Statistics software version 22.0 (IBM Corp., Armonk, NY, USA). A *t*-test was conducted on monthly paired data (Yang et al. 2018) for evaluating possible significant differences between the actual and estimated air pollutant levels as well as meteorological conditions.

Table 1 Outcomes obtained by testing the proposed estimate process

Pollutant	N ^a	Average current level		Average estimated level		R ^d	Statistical significance			
		C ^b	SD ^c	C	SD		Linear regression (ANOVA)		Independent variable	
							F	p	C ^e	p
SO ₂ ($\mu\text{g}/\text{m}^3$)	20	7.33	2.00	7.68	2.31	0.647	5.67	0.03	0.63	0.03
CO (mg/m^3)	20	0.20	0.07	0.28	0.15	0.645	12.80	0.00	1.31	0.00
NO ($\mu\text{g}/\text{m}^3$)	46	4.11	2.81	5.06	3.83	0.721	47.58	0.00	0.98	0.00
NO ₂ ($\mu\text{g}/\text{m}^3$)	46	21.56	6.39	24.71	6.57	0.888	163.93	0.00	0.91	0.00
PM _{2.5} ($\mu\text{g}/\text{m}^3$)	12	9.83	1.42	10.70	1.79	0.697	2.26	0.04	0.66	0.04
PM ₁₀ ($\mu\text{g}/\text{m}^3$)	24	20.51	5.20	22.99	3.9	0.647	11.52	0.00	0.68	0.00
O ₃ ($\mu\text{g}/\text{m}^3$)	26	70.03	9.25	75.14	6.87	0.791	33.54	0.00	0.59	0.00
C ₇ H ₈ ($\mu\text{g}/\text{m}^3$)	12	1.26	0.58	1.64	0.79	0.659	7.64	0.02	0.89	0.20
C ₆ H ₆ ($\mu\text{g}/\text{m}^3$)	12	0.22	0.10	0.24	0.10	0.797	17.42	0.00	0.78	0.00
TH (mg/m^3)	6	1.28	0.16	1.39	0.20	0.783	6.34	0.04	0.99	0.04
CH ₄ ($\mu\text{g}/\text{m}^3$)	6	1.10	0.20	1.23	0.14	0.841	9.45	0.37	0.63	0.03

^aNumber of paired samples

^bConcentration

^cStandard deviation

^dPearson's coefficient of correlation

^eCoefficient value of the independent variable

Results and discussion

Estimate of target air pollutant concentrations during the lockdown period

According to estimate process's sequence listed in Sect. 2 within Material and Methods, the monthly average concentrations for each target pollutant was estimated between January 2018 and February 2020. Table S5 shows Pearson's coefficients of correlation resulting when comparing the estimated and current monthly concentrations for each target pollutant and fixed measurement station in order to reflect the interrelation degree between them. As can be seen, Pearson's coefficients ranged from 0.650 to 0.970, reaching an average of 0.809 ± 0.114 .

In order to summarize the observed outcomes, polluting species were grouped by the type of station. So, monthly average time series concerning estimated and current levels for each investigated pollutant are represented from Fig. S3 to S5. Note that a similar profile for each pollutant between January 2018 and February 2020 is pictured, which provide consistence to the estimated levels along the shutdown period. Similarly, nonsignificant differences between the current and estimated monthly average concentrations for each pollutant were found when is applied a paired *T*-test.

To evaluate the developed estimate process's reliability, monthly average air pollutant levels obtained by the estimate model over July and August 2020 were compared against the actual monthly average concentrations using a simple linear regression test. Grouping all selected pollutants, the comparison exercise resulted in high concordance between estimated vs current pollutant levels (see Fig. 1). The linear regression model reached a Pearson's coefficient of 0.9902 (estimated level = $1.0571 \times$ actual level + 0.881, $N = 228$, $p < 0.001$), signaling that the independent variable accounts for 98.0% of the total variance of the dependent variable. It needs to be highlighted that the line equation of estimated and current concentrations proved in values close to 1 and lower than this one for the slope and intercept, respectively. Statistical analysis (ANOVA) of the linear regression equation displayed that the estimation analysis significantly enhances the forecasting of the dependent variable with a *F* value of 10,578.93 ($p = 0.00$). Similarly, ANOVA of the independent variable's regression coefficient indicated its significance and inclusion in the linear regression equation ($p = 0.00$). They were not found significant differences

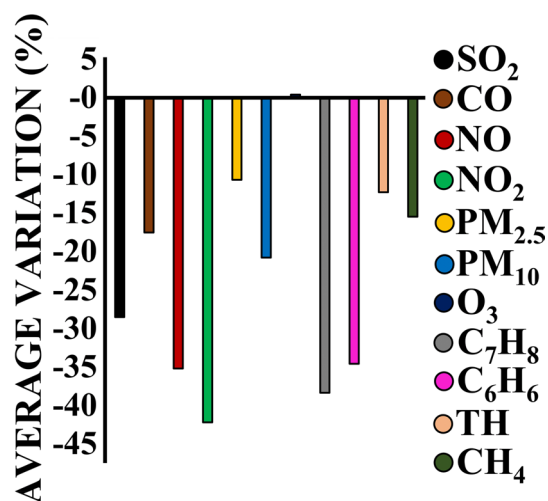


Fig. 2 Average variation of the air pollutant levels during the lockdown period in the researched domain

between paired samples of estimated and actual levels using the paired *t*-test.

While a global study exhibited a high-reliability degree regarding the used estimate process, Table 1 shows a statistical summary for each polluting species in order to provide a more detailed perspective. As it can be seen, Pearson's coefficients of correlation ranged between 0.645 (the independent variable explained 42% of the total variance of the dependent variable, in the case of CO) and 0.888 (79%, for NO₂). The rest of the pollutants displayed coefficients of correlation included in that interval.

In order to discern the validity of the estimate process applied to individual pollutants, Pearson's coefficient values are interpreted according to the proposal developed by Dancey and Reidy 2007. They classify as zero (value 0), weak (from ± 0.1 to ± 0.3), moderate (± 0.4 – 0.6), strong (± 0.7 – 0.9) and perfect (± 1) the association degree between two correlated variables. Thus, a more detailed analysis regarding the representativeness of the coefficients of correlation showed that 42% of cases fell into the interval moderate (although with values next to 0.7), while 58% exhibited a relationship strong, which revealed that there was a reasonable correlation strong between estimated and current air pollutant levels. Significant differences were not found between paired samples of estimated and actual levels using the paired *t*-test as the mean concentrations.

In conclusion, the previously exhibited evidence supports the simple linear regression-based models' applicability to estimate target air pollutant levels in ambient air, taking into account the stationarity index and time series trend, which is in line with the consideration reported by Zangari et al. 2020 respect to consider air quality trends when gauging short-term pollution changes.

Comparing current vs estimated polluting compound levels along the quarantine period

In order to appraise likely Madrid City's air quality changes between March and June 2020, the average variation of the current levels concerning estimated levels was evaluated in the function of (i) each target pollutant and (ii) the type of fixed measurement station.

Attending point (i), Fig. 2 represents the average variation on the ambient air of each target pollutant during the lockdown period. As a first reflection, it is essential to highlight that a decrease in the polluting levels in the target urban atmosphere, regardless of its quantitative value, was observed for all species during the quarantine period, except for ozone, which is in line with reported by Khan et al. 2021 and Rupani et al. 2020. Note that all compounds decreasing at the ambient level are considered primary air pollutants directly released by emission sources into the atmosphere. Although NO_2 is a secondary air pollutant, this one is yielded rapidly (within minutes) by reacting nitrogen monoxide and ozone (Lin et al. 2016). The primary pollutants' prevailing emission sources point mainly toward vehicular emissions and industrial activities, suffering a notable decline during the lockdown period. In the case of CH_4 , its major emission focuses drive to the energy, fossil combustible, incineration of wastes and landfills (EPA 2020).

Broadly, the reduction proportion concerning the air pollution level pre- and during the COVID-19 period varied between -40.0 and -10.1% (maximum and minimum drop, respectively). Whereas the drastically decreasing levels corresponded to nitrogen oxides (NOx : involving NO and NO_2) and volatile organic compounds (VOCs : encompassing C_6H_6 and C_7H_8) with mean values of 36.7% and 34.5% , respectively, a moderate abatement relapsed on CO , $\text{PM}_{2.5}$, PM_{10} , CH_4 and TH reaching mean declines lower than 17% . As an intermediate stage, SO_2 decreased 27% .

In the case of particulate matter, it is necessary to mention that the quarantine period's impact on ambient pollution

level variation was differential in relied on particulate size. Thus, the particles with an aerodynamic diameter up to $10\ \mu\text{m}$ lowered their concentration twice more than those with a diameter of less than 2.5 .

To elucidate whether changes in pollution levels regarding the time variable were similar to all chemical species, Fig. S6 pictures the occurring average decreases per target pollutant along the shutdown months. Broadly, a rapid abatement in March and April is evidenced, except for ozone. Moderate restrictive measures implanted in March reflected abrupt SO_2 , NOx and VOCs levels changes, while that severe restrictive measures in April produced the highest decreases. Then, when gradually relaxing confinement measures (May and June), the reduction was lower than the previous months, thereby corroborating a link between human activities and polluting levels in the ambient air, except TH and CH_4 exhibiting consistently progressive decreases from March to June.

Ozone deserves special attention; given that it is the one pollutant rising its ambient air concentration during the restriction measure outbreak. It is a secondary air pollutant yielded from chemical reactions among other atmospheric compounds, generally primary pollutants. In this sense, NOx and VOCs are precursors of the ground-level ozone (Suarez-Bertoa et al. 2015), and its formation is consistently dependent on the photochemical NOx/VOCs ratio (Deng et al. 2019). While benzene, toluene, ethylbenzene and xylene account for about 95% of the total VOCs (Zhao et al. 2011), benzene is considered the major contributor to O_3 formation (Xu et al. 2018). In the investigated urban atmosphere, the O_3 level was sustained along the restriction period, exhibiting a slight rise next to 0.4% . Several reasons might explain this fact. Firstly, at the level urban, tropospheric O_3 can be more limited by VOCs than NOx , and therefore, an abatement in NOx emissions would raise ground-level O_3 concentration unless VOCs are reduced at a higher rate simultaneously (Kerimray et al. 2020). Based on the reductions of the ambient levels observed in the studied atmosphere for NO (33.3%), NO_2 (40.0%), C_6H_6 (32.8%) and C_7H_8 (36.3%), it can be assumed a decrease slightly higher in NOx than VOCs emissions due to the severe restrictive measures during the lockdown period. Secondly, ground-level O_3 concentrations are inversely proportional to NOx concentrations as a consequence of titration chemistry (Sharma et al. 2016). Whereas NO_2 helps in O_3 formation, the titration effect of NO is an important way of O_3 consumption in

Table 2 Urban air quality changes derived from COVID-19 implanted measures reported on other studies worldwide

Studied area	Studied period (2020)	Air pollutant (Variation, %)	References
Tehran (Iran)	21st March–21st April	SO ₂ (between – 5 and – 28) NO ₂ (between – 1 and – 33) CO (between – 5 and – 41) PM ₁₀ (between – 1.4 and – 30) O ₃ (between + 0.5 and + 103) PM _{2.5} (between + 2 and + 50)	(Broomandi et al. 2020)
Northern China (44 cities)	1–21st January	SO ₂ (– 6.76), PM _{2.5} (– 5.93), PM ₁₀ (– 13.66), NO ₂ (– 24.67) and CO (– 4.58)	(Bao and Zhang 2020)
Sau Paulo (Brasil)	In late March	CO (up to – 64.8), NO (up to – 77.3) NO ₂ (up to – 54.3) and O ₃ (~ + 30)	(Nakada and Urban 2020)
New York City (United States)	March–May	PM _{2.5} (– 36) and NO ₂ (– 51)	(Zangari et al. 2020)
Wuham (China) Daegu (South Korea) Tokyo (Japan)	23rd January–8th April 23rd February (self-reflection) 25th March (self-reflection)	PM _{2.5} (– 29.9) NO ₂ (– 53.2) PM _{2.5} (– 20.9) NO ₂ (– 19.0) PM _{2.5} (– 3.6) NO ₂ (– 10.4)	(Ma and Kang 2020)
Singapore	7th April–11th May	PM ₁₀ (– 23), PM _{2.5} (– 29), NO ₂ (– 54), CO (– 6), SO ₂ (– 52) and O ₃ (+ 18)	(Li and Tararini, 2020)
Quito (Ecuador)	17 th March–12 th April	NO ₂ (– 68), SO ₂ (– 48), CO (– 38) and PM _{2.5} (– 29)	(Zalakeviciute et al. 2020)
Delhi (India)	24th March–14th April	PM ₁₀ and PM _{2.5} (– > 50), NO ₂ (– 52.68) and CO (– 30.35)	(Mahato et al. 2020)
Auckland (New Zealand)	27th Mach–17th April	NO ₂ (between – 34 and – 57) BC (between – 55 and – 75) PM _{2.5} (between – 8 and – 17) PM ₁₀ (between – 7 and – 20) O ₃ (+ 16.7)	(Patel et al. 2020)
Metropolitan City of Milan (Italy)	Partial lockdown: 9th–22nd March Total lockdown: 23rd March–5th April	PM ₁₀ (between – 32.7 and – 40.5) PM _{2.5} (between – 37.1 and – 44.4) C ₆ H ₆ (~ – 49), CO (~ – 45), SO ₂ (– 19.9), NO ₂ (– 40) and O ₃ (> 2 times) PM ₁₀ (between – 13.1 and – 18.9) PM _{2.5} (between – 47.1 and – 47.4) C ₆ H ₆ (> – 65), SO ₂ (– 6.8), NO ₂ (– 59) and O ₃ (> 2.9 times)	(Collivignarelli et al. 2020)
India (22 cities)	16th March–14th April	Overall, PM _{2.5} (– 43), PM ₁₀ (– 31), CO (– 10), NO ₂ (18), O ₃ (+ 17) and SO ₂ (negligible)	(Sharma et al. 2020)
Unites States (28 cities)	15th March–25th April	NO ₂ (between – 5 and – 49) CO (between + 1 and – 37) PM _{2.5} (between + 112 and – 45) PM ₁₀ (between + 29 and – 57) O ₃ (between + 25 and – 17)	(Chen et al. 2020)
Hangzhou (China)	4–18th February	PM ₁₀ (– 58), PM _{2.5} (– 47), NO _x (– 83), SO ₂ (– 11), CO (– 30) and O ₃ (between + 102 and + 125)	(Yuan et al. 2021)
Gujarat state (India)	24th March–20th April	PM _{2.5} (between – 38 and – 78) PM ₁₀ (between – 32 and – 80) NO ₂ (between – 30 and – 84) CO (between – 3 and – 55) O ₃ (between + 16 and + 48)	(Selvam et al. 2020)



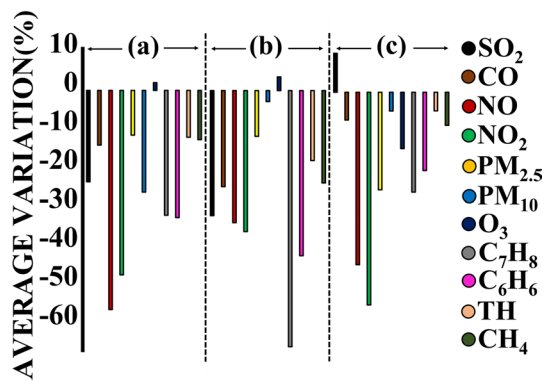


Fig. 3 Average variation of each pollutant per fixed monitoring station. Key: (a) Urban traffic station, (b) urban background station (c) suburban background station

urban condition, and thus, the titration chemistry can reduce its concentration at the tropospheric level (Pei et al. 2020). Therefore, decreasing NO levels restricts the titration process, limiting O_3 accumulation inhibition. This finding is in line with that reported by (Huang et al. 2021), informing that a large decrease in NOx emissions from the transport sector increases ozone levels. Besides, the moderate diminution of $PM_{2.5}$ fraction (~10%) favors the increase in O_3 levels during the lockdown period (Li et al. 2019a, b).

Given the valuable findings reported by other authors within the objective planted in this work, searching for possible urban environment patterns results in a remarkable subject. In this sense, Table 2 shows different outcomes relative to urban air quality changes due to the lockdown period implanted in other domains of study. Qualitatively, this work's exhibited results are in line with those shown in Table 2, with broad air pollutants decrease except for O_3 . Nevertheless, at the quantitative level, that variation is supported in a wide value interval, dependent on both the urban location and lockdown period. Therefore, air quality changes due to shutdown measures implanted in other urban environments, as a consequence of the COVID-19 pandemic, do not sustain a common pattern, which might be relevant in terms of air quality management policies in urban zones globally.

On a large scale, Metya et al. 2020 researched potential air pollutant changes derived from implementing restrictive measures in India and China, reporting lower decreasing levels than those observed in this work (−17% for NO_2 and SO_2 in India and Eastern India, respectively, and −25% and −6.5% for NO_2 and CO in China and North-Central China, respectively). Similarly, based on observations from

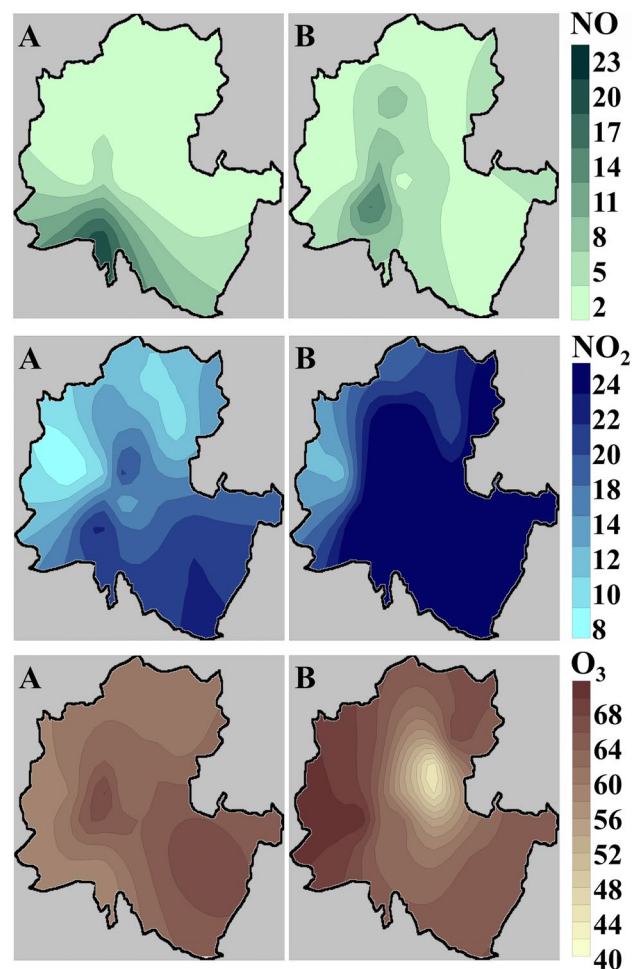


Fig. 4 Spatial distribution gradient of NO, NO_2 and O_3 during the lockdown period across target surface (Unit: $\mu g/m^3$). Note: A: Mean current concentrations and B: Mean estimated concentrations

the Copernicus Sentinel-5P satellite, the European Space Agency evaluated air quality changes brought on by strict COVID-19 measures in major European cities (Milan, Madrid, Paris, Berlin and Budapest), reporting dissimilar decreases. In particular, Madrid city exhibited a NO_2 reduction of close to 50% (see https://www.esa.int/Applications/Observing_the_Earth/Copernicus/Sentinel-5P/Air_pollution_in_a_post-COVID-19_world, accessed January 25, 2021). Whereas this lookout was obtained by comparing 2019 and 2020 "in situ" observations, this work compared current and estimated values during the lockdown period. For this reason, a NO_2 drop slightly lower (40%) than that reported by the European Space Agency was observed, which is in concordance with the clearly down trend of the

NO_x emissions in Madrid city, reducing up to 49.9% from 1999 to 2017 (IAPM 2019).

Up to here, each pollutant has been respected at the individual level to know average changes in studied urban pollution, which is relevant in terms of air quality management at the global level in the target domain. Nevertheless, a disaggregated approach would provide a more detailed knowledge concerning air quality variations per zones within the target urban environment. To achieve this objective, they were addressed individual evaluations based on the type of fixed measurement station (point (ii)), which could help focus and direct efforts to improve the air quality management within a context of limited resources.

In this sense, Fig. 3 exhibits the percentage change concerning each pollutant's average level per type of fixed station. Note that there is not a standard behavior among all compounds. Thus, SO₂, CO, C₇H₈, C₆H₆, TH and CH₄ variations are consistently dependent on the fixed station location, displaying the highest decreasing levels at urban against suburban stations, especially for urban background sites. Whereas similar decreases in PM_{2.5} particles and O₃ leads to urban stations, the highest diminishment appears in suburban zones, as urban traffic sites in the case of NO and PM₁₀ particles. In a particular instance, NO₂ is the only pollutant, keeping variations reasonably similar at the types of evaluated stations. Therefore, without recounting NO₂, 60% of target species exhibited the highest decreasing levels in urban background areas, while urban traffic sites and suburban background zones accounted for 20% each.

Geospatial analysis

Broadly, while a decreasing trend for researched pollutants over the quarantine period has been revealed, except for ozone, it is pertinent to assess the spatial gradient across researched Madrid city's surface regarding pollution distribution information. Among the total of researched polluting compounds, they were addressed those pollutants measured in a minimum of 10 fixed monitoring stations.

Figure 4 represents the spatial NO, NO₂ and O₃ gradient concerning concentration averaged from March to June 2020. As it can be seen, the variation on the NO levels evidenced in Results' point 2 is translated into a distinct geospatial pattern when comparing current vs estimated concentrations, thereby confirming a change in the distribution gradient of this pollutant due to the implanted measures during the shutdown period. The highest concentrations of

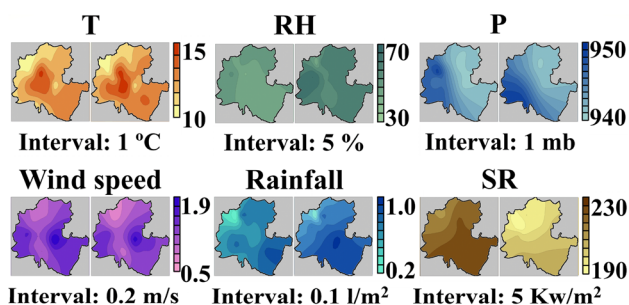


Fig. 5 Average spatial distribution gradient of target meteorological variables between January and June 2019 and 2020, respectively. Key: T: Temperature, RH: Relative humidity, P: Barometric pressure and SR: Solar radiation. Note: The maps pictured in the right column correspond to 2019 as the left column to 2020

estimated NO are found in the South, North and East zones, while the highest real levels comprise areas encompassing the South-West to South-East zone. However, the same geospatial distribution for NO₂ is supported, in the sense that the axis picturing gradient from highest to lowest concentration is prolonged from South-East to North-West for both sceneries (current and estimated levels). In order to offer an overview concerning spatial distribution of pollutant emissions of nitrogen oxides along the target surface, a distribution gradient map is showed in Fig. S7.

As expected, geospatial O₃ analysis concludes in a deep variation about the distribution real and estimated concentrations gradient of this compound along the selected surface, motivated by changing levels of their precursor pollutants. In this sense, the highest estimated O₃ concentrations are located in the West zone, as the lowest levels in the Central area, contrary to NO and NO₂. Nevertheless, attending current levels, the highest and lowest O₃ concentrations are sited in South-East and Center zones, thereby confirming that restriction measures implanted resulted in different geospatial O₃ pattern.

Concerning CO and PM₁₀, distribution gradient similar between the current and estimated stage setting is exhibited, with the lowest CO levels pictured in the West zone and a decrease of current and estimated PM₁₀ concentrations from the East zone toward the West zone (see Fig. S8). For SO₂, slight discrepancies concerning geospatial analysis are appraised. The estimated concentrations diminish from the Central zone toward the rest of the surface with minimum values in the West zone. At the same time, although the lowest concentrations are sustained in the West zone, the current levels decrease from the South zone.

Possible influence of emission sources and meteorological variables on air quality changes

Relative to emission sources, given that the study is focused on an urban environment, the most prevailing emission air pollutant sources drive vehicular emissions. In this context, and attending the number of circulating vehicles on Madrid city's surface, Fig. S9 pictures the traffic intensity trend from January 2018 to June 2020, expressed as a monthly average. It is paramount to highlight that the number of monthly average vehicles draws a similar profile along 2018 and 2019, reflecting an annual average value practically equal for both annuities. It can be seen as August offers minimum values due to being a holiday period.

From January to June 2020, this tendency is sustained during the two first months with a mean value of 2,208,483 vehicles, followed by a significant reduction (number of average vehicles between March and June 2020: 1,026,645).

At averaging data of the traffic intensity during March, April, May and June 2018 and 2019, respectively, with the same months in 2020, a drastic decrease in the vehicle's number is observed. This abatement is produced rapidly for the three first months and moderately during June (March: a drop of 42%, April: 78%, May: 61% and June: 27%).

Based on the previous evidence, it can be concluded that a similar pattern regarding Madrid city's traffic intensity between January 2018 and February 2020 is sustained. Nevertheless, this behavior experiences a profound decreasing change coinciding with implementing measures for avoiding the COVID-19 spread. Therefore, the notable abatement in the Madrid city's traffic load, due to the severe restrictive measures implemented during the lockdown period, can be linked to the generalized decrease of target air pollutants assessed in this study.

Relative to meteorological variables, the behavior of these parameters between January and June 2019 and 2020, respectively (data for 2018 not available), were compared in order to elucidate whether possible pattern changes in these might justify the decreasing air quality changes evidenced in the investigated urban environment. In reliance on this objective, data recorded by each monitored meteorological point were respected. In this sense, the meteorological features' mean values embracing the target period are shown in Fig. S10. As can be seen, the pictured meteorological features show clearly similar qualitative behavior between January and June 2019 and 2020, respectively. Some variables exhibit analogous profiles, reflecting quite similar mean values between both investigated periods relative to quantitative arguments. Thus, mean temperature values of 13.4 °C (from

January to June 2019) and 13.6 °C (from January to June 2020), 0.7 and 0.9 l/m² for the rainfall, and 1.4 and 1.3 Kw/m² for the solar radiation were observed, illustrating slight variations (~ 10%) for the rest of meteorological variables (48.3 and 60.7% for the relative humidity, 4.0 and 3.5 mb for the atmospheric pressure, 222.7 and 190.8 Kw/m² for the solar radiation). By applying a *t*-test on monthly paired data for each meteorological variable (January and June 2019 and 2020, respectively), difference significates were not found.

Although the meteorological features monitored at each control station displayed a reasonably similar behavior between January and June 2019 and 2020, respectively, the distribution gradient of those variables across the researched domain must be evaluated for corroborating that this pattern also is attributable at the spatial level. In this sense, Fig. 5 represents the spatial distribution of meteorological conditions along Madrid city's investigated area. Each variable's mean values from January to June 2019 and 2020, respectively, were respected to build meteorological maps. Broadly, spatial gradients exhibited for 2020 for each variable were similar to those pictured for 2019. A linear regression analysis between the meteorological dataset was run in order to quantify the spatial similarity percentage reached between both years (Galán-Madruga 2021). The outcomes showed Pearson's coefficients of correlation higher than 0.5 for all meteorological features, following the sequence: wind speed ($r = 0.980$, $N = 10$, $p < 0.001$), temperature ($r = 0.854$, $N = 19$, $p < 0.001$), relative humidity ($r = 0.794$, $N = 18$, $p < 0.001$), atmospheric pressure ($r = 0.760$, $N = 8$, $p < 0.02$), rainfall ($r = 0.701$, $N = 9$, $p < 0.02$) and solar radiation ($r = 0.551$, $N = 7$, $p < 0.1$), thereby confirming a reasonably similar spatial gradient for the first semester 2019 and 2020, respectively.

At comparing the spatial distribution exhibited during the investigated period in 2019 and 2020, it is observed that higher temperature levels fell into the target domain's Central zone, while wind speed and relative humidity pointed toward East and West areas, respectively. Higher rainfall and solar radiation levels were found in the South zone, whereas the West zone highlighted for the atmospheric pressure.

The wind direction is a meteorological feature playing a relevant role in the dispersion and dilution of polluting compounds into the air matrix. For this reason, its study results primordial within the planted context. This variable is expressed in degrees, counted in the clockwise direction from geographic north, assigning to this point the value of 0 degrees, as 90, 180 and 270 degrees to the East, South and West, respectively. It indicates the wind entrance course on the study surface.



Fig. S11 pictures mean values of wind direction in terms of the total and monthly period, respectively, during the investigation. Note that a reasonable similar qualitative outline is represented in 2019 and 2020 ($r=0.611$, $N=10$, $p<0.02$). The wind direction's comparative study between January and June 2019 and 2020, respectively, shows quantitative differences, averaging values of 161.7 degrees (2019) and 109.5 degrees (2020). However, those results are translated in a prevailing global wind from the Southeast, coinciding to the second quadrant, according to the possible wind directions (North/East: 1st quadrant, East/South: 2nd quadrant, South/West: 3rd quadrant and West/North: 4th quadrant). Attending each meteorological control station's mean value along the studied period, the number of times the wind direction fell into the 2nd quadrant was 70 and 80% (2019 and 2020, respectively, see Fig. S12).

Based on previous outcomes, the meteorological conditions were sustained in 2019 and 2020 under reasonably similar records, concluding that those variables were not responsible for the reducing changes in the target surface's air quality occurred in lockdown time.

In order to evaluate the influence of meteorological features on target air pollutants over the lockdown period, a simple linear regression analysis between each polluting and each meteorological variable was conducted. For running this test, monthly average data (relative to pollutants and weather conditions), encompassing from March to June 2020 were employed.

In this context, Pearson's coefficients of correlation resulting are shown in Table S6. To better interpret the

obtained relationships, a Pearson's coefficient higher than 0.7 was selected as a cutoff value (Dancey and Reidy 2007). Broadly, the impact of the meteorological variables on pollutants along the target period showed the next sequence: wind direction (strong association with 7 pollutants), wind speed, temperature, solar radiation and rainfall (5 pollutants), relative humidity (3 pollutants) and, finally, pressure (1 pollutant). Considering each pollutant, the most affected chemical species by the weather conditions were CH_4 and TH (5 meteorological variables, named: wind direction, temperature, relative humidity, solar radiation and rainfall), while O_3 was influenced by wind direction, temperature, relative humidity and solar radiation, and C_6H_6 and CO by the wind direction, temperature and solar radiation. Finally, the rest of the pollutants were mainly affected by two meteorological variables, wind speed and direction in the case of nitrogen oxides and wind speed and rainfall for SO_2 , PM_{10} and C_7H_8 .

At considering the cases of strong correlation (>0.7), positive and negative associations were exhibited for the wind speed and direction variable, respectively, while that temperature, solar radiation and rainfall showed negative correlations for the most of pollutants. O_3 regressions (>0.7) displayed contrary trends concerning the rest of pollutants, exhibiting negative association degrees with relative humidity variable and positive for wind direction, temperature and solar radiation.

In relation to the outcomes reached concerning the study "air pollutants vs meteorological variables" conducted in this work over the quarantine period, other investigations within the target frame were consulted in order to illustrate or not

Table 3 Outcomes of PCA technique and PCA-MLR analysis

Independent variable	Factor loadings resulting of PCA analysis				Results of combined PCA-MLR technique			
	2019		2020		2019		2020	
	PC1	PC2	PC1	PC2	PC1 (%)	PC2 (%)	PC1 (%)	PC2 (%)
Road traffic (number of vehicles)	0.340	0.863	-0.253	0.910	1.5	9.0	4.0	6.5
Wind speed	0.894	0.427	0.577	-0.644	10.2	2.2	8.0	0.1
Wind direction	-0.177	0.663	-0.608	0.732	0.4	5.3	8.7	1.1
Temperature	0.979	-0.039	0.964	-0.165	12.2	0.0	12.9	0.0
Relative humidity	- 0.912	0.357	- 0.994	0.051	10.6	1.5	12.6	0.5
Pressure	-0.617	-0.674	-0.343	0.774	4.9	5.5	4.9	8.8
Solar radiation	0.989	-0.054	0.944	-0.272	12.5	0.0	13.3	0.1
Rainfall	-0.218	0.882	-0.223	- 0.969	0.6	9.4	0.2	8.0

Higher factor loadings are remarked in bold



potential similarities. Although some researcher groups linked meteorological variables to COVID-19 cases, in terms of incidence (Kolluru et al. 2021; Tello-Leal et al. 2021), other ones laid down associations between air pollutants and weather conditions over a specific lockdown period. So, Gao et al. 2021 assessed potential variations on air quality in 4 Chinese megacities (Wuhan, Beijing, Shanghai and Guangzhou) during the COVID-19 lockdown. Among other factors, they studied the relationship between air pollutants ($PM_{2.5}$, NO_2 and SO_2) and meteorological conditions (precipitation, temperature, relative humidity, wind speed and boundary layer height). Broadly, they observed that most of the meteorological conditions were negatively correlated with target air compounds. In this study, while the rainfall and relative humidity variables showed negative correlations for the three air pollutants studied by Gao et al. 2021, except for the association between NO_2 and relative humidity, the wind speed was positively correlated. Particularly, Gao et al. 2021 observed that the temperature had a stronger negative influence on $PM_{2.5}$ in comparison with NO_2 and SO_2 in all four target Chinese cities, while this research reflected a higher correlation degree for SO_2 than for NO_2 and $PM_{2.5}$. Similarly, Zhou et al. 2021 observed distinct influences of temperature on air pollutants. While it had significant and negative correlations with SO_2 and NO_2 , positive associations were probed with $PM_{2.5}$, PM_{10} and CO. This study resulted in positive and negative correlations for SO_2 , PM_{10} and $PM_{2.5}$, and NO_2 and CO, respectively.

Based on the previous evidence, a common pattern relative to the influence of meteorological conditions on air quality variations over quarantine periods implanted in different geographic zones is not sustained. This situation has also been evidenced over periods without lockdown period. So, Yang et al. 2020 assessed the influence of determining factors of $PM_{2.5}$ pollution, meteorological features among others, in 368 cities and 9 urban agglomerations over Chinese in 2015. They concluded that the impact of meteorological factors on $PM_{2.5}$ concentrations was complicated in terms of spatial variations.

The occurrence of polluting compounds into the atmosphere depends on both emissions sources (anthropogenic and natural) and factors relating to meteorological conditions and topographic features. Although the emissions released by anthropogenic sources, largely responsible for the emergence of pollutants in the air matrix, decreased when limiting human activity over the lockdown period, the rest of the variables play a primordial role in the presence of pollutants in the ambient air. These variables, together, are specific for each terrestrial zone, which hinders the search of patterns within the framed objective.

Up to here, it has been individually studied a possible influence of road traffic and meteorological pattern on the abatement of the air pollutant levels in Madrid City. Nevertheless, given that both variables simultaneously act on the air mixtures, a joint study is addressed, executing a combined PCA-MLR analysis according to Sect. 4 of Materials and Methods. Table 3 shows the outcomes reached by using combined PCA-MLR analysis. Relative to the results achieved in applying the PCA technique, the total of variables were compressed into two components (PC1 + PC2), accounting for 85.94% (2019) and 89.53% (2020) of the initial data package variance. A more detailed analysis exhibited that PC1 explained 52.91% (2019) and 64.42% (2020) of the original total information, as 33.03% (2019) and 25.12% (2020) in the case of PC2. Regardless of the year, the major components (PC1) were highly loaded with common variables such as temperature, relative humidity and solar radiation. Besides, the wind speed in 2019 was a dominant factor loading, while it was shared between PC1 and PC2 in 2020. Similarly, Table 3 shows the outcomes obtained by using combined PCA-MLR analysis. According to the PCA-MLR study's outcomes, each variable's total contribution to the original information package is reasonably similar to both years, thereby ratifying the set of variables' same pattern in both years (see Fig. S13). Although the total influence of road traffic is similar to both years, note that it is almost 4 times higher in 2020 than in 2019 (see PC1 values in results of combined PCA-MLR technique in Table 3).

Conclusion

The quick person to person transmission of new coronavirus (SARS-CoV-2) urged numerous worldwide countries to implanted severe shutdown measures, which would offer a unique opportunity in order to understand and value the impact of those actions on air quality, particularly to urban environments, given the high pollution load occurring in those areas. Within this frame, a South Europe capital was respected as a case study. An original dataset consisting of polluting 11 species commonly monitored in urban environments was the basis of this work and acquired from the Municipality of Madrid's open data portal.

As an innovative viewpoint concerning other valuable research's focusing on the same planted objective, the present study's scope pretends to explain urban air quality changes in terms of the involved whole urban surface and disaggregated by internal zones. In this sense, although the



influence of the COVID-19 lockdown on the target urban atmosphere was not similar across the researched domain, it showed widespread declines. The shutdown period on polluting load changes depended on the monitored zones within the target urban environment, which revealed distinct consequences on atmospheric pollution across the researched domain, except for NO₂, keeping decreases practically similar to all measurement sites. In this sense, the most prominent drops concerning air pollutant levels relapsed on zones cataloged as urban sites, such as urban background locations for SO₂, CO, C₆H₆, C₇H₈, TH and CH₄, and urban traffic sites for NO and PM₁₀. For PM_{2.5} and O₃, it is exhibited the highest declines in zones considered as suburban sites.

The atmospheric reply to the strict confinement measures did not keep the same behavior for all polluting species in quantitative valuation. While the highest abatement levels pointed to NO_x and VOCs, attaining values higher than 35%, the polluting diminution of the rest of the evaluated compounds fell into the 10–30% interval, except for O₃ showed a slight rise of 0.4%. Nevertheless, at the geospatial level, those substantial changes in atmospheric levels mitigation were not translated in variations regarding spatial distribution gradient of targeted air pollutants, except for NO, O₃ and SO₂, whose spatial gradients underwent a moderate and remarkable transformation, respectively.

Based on the previous evidence, the COVID-19 lockdown supports the link between target urban air pollution changes and the COVID-19 pandemic's containment measures implanted over the shutdown period, resulting in improved air quality. Although it was not attributable to potential variations in meteorological conditions, concerning the previous year, as a possible dilution effect on atmospheric pollution load, it was in line with the traffic intensity reduction.

Quantitatively comparing the study's outcomes with the meritorious findings reported by other authors, the same air pollutants behavior in response to the shutdown measures implanted in different urban environments is not sustained, thereby confirming the necessary to be done more exhaustive examinations on each urban environment. On the other hand, the influence of meteorological features on polluting compound levels' changes evaluated within the target atmosphere over the lockdown period did not display a common pattern at comparing with other geographic zones. Nevertheless, the outcomes reached in the studied domain might help manage urban air quality and future policy-making to mitigate punctual contamination episodes.

Supplementary Information The online version contains supplementary material available at <https://doi.org/10.1007/s13762-022-04464-6>.

Acknowledgements The original dataset was published online by the Municipality of Madrid through its open database portal (<https://madrid.es/>). This data package constituted the basis of this research. The author thanks the local government for the transparency policy set concerning the use and spread of data (more information in <https://transparencia.madrid.es/portal/site/transparencia>, accessed January 27, 2020).

Author contributions DGM: was responsible for the conceptualization, resources, methodology, formal analysis, writing the original paper and editing.

Funding No funding was received.

Declarations

Conflict of interest The author declares that there are no conflicts of interest. This research does not have commercial purposes, only scientific ones. This research did not receive any specific grant from funding agencies in the public, commercial or not-for-profit sectors.

References

- Andersen KG, Rambaut A, Lipkin WI, Holmes EC, Garry RF (2020) The proximal origin of SARS-CoV-2. *Nat Med* 26:450–452. <https://doi.org/10.1038/s41591-020-0820-9>
- Bao R, Zhang A (2020) Does lockdown reduce air pollution? Evidence from 44 cities in northern China. *Sci Total Environ* 731:139052. <https://doi.org/10.1016/j.scitotenv.2020.139052>
- Barman U, Choudhury RD (2020) Smartphone image based digital chlorophyll meter to estimate the value of citrus leaves chlorophyll using linear regression, LMBP-ANN and SCGBP-ANN. *J King Saud Univ Comp Info Sci*. <https://doi.org/10.1016/j.jksuci.2020.01.005>
- Beauchamp M, Malherbe L, de Fouquet C, Létinois L, Tognet F (2018) A polynomial approximation of the traffic contributions for kriging-based interpolation of urban air quality model. *Environ Model Soft* 105:132–152. <https://doi.org/10.1016/j.envsoft.2018.03.033>
- Bherwani H, Gautam S, Gupta A (2021) Qualitative and quantitative analyses of impact of COVID-19 on sustainable development goals (SDGs) in Indian subcontinent with a focus on air quality. *Int J Environ Sci Technol*. <https://doi.org/10.1007/s13762-020-03122-z>
- Bigdeli M, Taheri M, Mohammadian A (2021) Spatial sensitivity analysis of COVID-19 infections concerning the satellite-based four air pollutants levels. *Int J Environ Sci Technol* 18:751–760. <https://doi.org/10.1007/s13762-020-03112-1>
- Broomandi P, Karaca F, Nikfal A, Jahanbakhshi A, Tamjidi M, Kim JR (2020) Impact of COVID-19 event on the air quality in Iran. *Aerosol Air Qual Res* 20:1793–1804. <https://doi.org/10.4209/aaqr.2020.05.0205>
- Chen Y, Zhang L, Zhao B (2019) Identification of the anomaly component using BEMD combined with PCA from element concentrations in the Tengchong tin belt, SW China. *Geosci Front* 10:1561–1576. <https://doi.org/10.1016/j.gsf.2018.09.015>
- Chen LWA, Chien LC, Li Y, Lin G (2020) Nonuniform impacts of COVID-19 lockdown on air quality over the United States. *Sci Total Environ* 745:141105. <https://doi.org/10.1016/j.scitotenv.2020.141105>



- Collivignarelli MA, Abbà A, Bertanza G, Pedrazzani R, Ricciardi P, Miino MC (2020) Lockdown for CoViD-2019 in Milan: What are the effects on air quality? *Sci Total Environ* 732:139280. <https://doi.org/10.1016/j.scitotenv.2020.139280>
- Dancey CP, Reidy J (2007) *Statistics without Maths for Psychology*. Pearson Education
- Deng Y, Li J, Li Y, Wu R, Xie S (2019) Characteristics of volatile organic compounds, NO₂, and effects on ozone formation at a site with high ozone level in Chengdu. *J Environ Sci* 75:334–345. <https://doi.org/10.1016/j.jes.2018.05.004>
- EPA (2020) Unites States environmental protection agency. Inventory of U.S. Greenhouse Gas Emissions and Sinks 1990–2018. EPA 430-R-20–002. <https://www.epa.gov/sites/production/files/2020-04/documents/us-ghg-inventory-2020-main-text.pdf>. Accessed 9 Jan 2021
- Faridi S, Yousefian F, Niazi S, Ghalhari MR, Hassanvand MS, Naddafi K (2020) Impact of SARS-CoV-2 on ambient air particulate matter in Tehran. *Aerosol Air Qual Res* 20:1805–1811. <https://doi.org/10.4209/aaqr.2020.05.0225>
- Galán-Madruga D (2021) A methodological framework for improving air quality monitoring network layout. Applications to environment management. *J Environ Sci* 102:138–147. <https://doi.org/10.1016/j.jes.2020.09.009>
- Gao C, Li S, Liu M, Zhang F, Achal V, Tu Y, Zhang S, Cai C (2021) Impact of the COVID-19 pandemic on air pollution in Chinese megacities from the perspective of traffic volume and meteorological factors. *Sci Total Environ* 773:145545. <https://doi.org/10.1016/j.scitotenv.2021.145545>
- Huang X, Tang G, Zhang J, Liu B, Liu C et al (2021) Characteristics of PM_{2.5} pollution in Beijing after the improvement of air quality. *J Environ Sci* 100:1–10. <https://doi.org/10.1016/j.jes.2020.06.004>
- IAPM (2019) Inventory of Madrid city air pollutant emissions 2017. Summary of emissions in the period 1999–2017. Directorate General for Sustainability and Environmental Control. <https://transparencia.madrid.es/UnidadesDescentralizadas/Sostenibilidad/EspeInf/Energia/CC/04CambioClimatico/4aInventario/Ficheros/Emissions/Inv2017.pdf>. Accessed 25 Jan 2021
- Karagulian F, Belis CA, Dora CFC, Prüss-Ustün AM, Bonjour S, Adair-Rohani H, Amann M (2015) Contributions to cities' ambient particulate matter (PM): a systematic review of local source contributions at global level. *Atmos Environ* 120:475–483. <https://doi.org/10.1016/j.atmosenv.2015.08.087>
- Kerimray A, Baimatova N, Ibragimova OP, Bukenov B, Kenessov B et al (2020) Assessing air quality changes in large cities during COVID-19 lockdowns: the impacts of traffic-free urban conditions in Almaty. *Kazakhstan Sci Total Environ* 730:139179. <https://doi.org/10.1016/j.scitotenv.2020.139179>
- Khan I, Shah D, Shah SS (2021) COVID-19 pandemic and its positive impacts on environment: an updated review. *Int J Environ Sci Technol* 18:521–530. <https://doi.org/10.1007/s13762-020-03021-3>
- Kolluru SSR, Patra AK, Nazneen NSMS (2021) Association of air pollution and meteorological variables with COVID-19 incidence: evidence from five megacities in India. *Environ Res* 195:110854. <https://doi.org/10.1016/j.envres.2021.110854>
- Kottek M, Grieser J, Beck C, Rudolf B, Rubel F (2006) World Map of the Köppen-Geiger climate classification updated. *Metz* 15:259–263. <https://doi.org/10.1127/0941-2948/2006/0130>
- Li J, Tararini K (2020) Changes in air quality during the COVID-19 lockdown in Singapore and associations with human mobility trends. *Aerosol Air Qual Res* 20:1748–1758. <https://doi.org/10.4209/aaqr.2020.06.0303>
- Li K, Jacob DJ, Liao H, Shen L, Zhang Q, Bates KH (2019a) Anthropogenic drivers of 2013–2017 trends in summer surface ozone in China. *Proc Natl Acad Sci USA* 116:422–427. <https://doi.org/10.1073/pnas.1812168116>
- Li W, Peng M, Wang Q (2019b) Improved PCA method for sensor fault detection and isolation in a nuclear power plant. *Nucl Eng Technol* 51:146–154. <https://doi.org/10.1016/j.net.2018.08.020>
- Li L, Li Q, Huang L, Wang Q, Zhu A et al (2020) Air quality changes during the COVID-19 lockdown over the Yangtze River Delta Region: an insight into the impact of human activity pattern changes on air pollution variation. *Sci Total Environ* 732:139282. <https://doi.org/10.1016/j.scitotenv.2020.139282>
- Lin C, Feng X, Heal MR (2016) Temporal persistence of intra-urban spatial contrasts in ambient NO₂, O₃ and Ox in Edinburgh, UK. *Atmos Pollut Res* 7:734–741. <https://doi.org/10.1016/j.apr.2016.03.008>
- Ma CJ, Kang GU (2020) Air quality variation in Wuhan, Daegu, and Tokyo during the explosive outbreak of COVID-19 and its health effects. *Int J Environ Res Public Health* 17:4119. <https://doi.org/10.3390/ijerph17114119>
- Mahato S, Pal S, Ghosh KG (2020) Effect of lockdown amid COVID-19 pandemic on air quality of the megacity Delhi. *India Sci Total Environ* 730:139086. <https://doi.org/10.1016/j.scitotenv.2020.139086>
- Marinello S, Lolli F, Gamberini R (2020) Roadway tunnels: a critical review of air pollutant concentrations and vehicular emissions. *Trans Res Part d: Trans Environ* 86:102478. <https://doi.org/10.1016/j.trd.2020.102478>
- Mayer H (1999) Air pollution in cities. *Atmos Environ* 33:4029–4037
- Metya A, Dagupta P, Halder S, Chakraborty S, Tiwari YK (2020) COVID-19 lockdowns improve air quality in the South-East Asian Regions, as seen by the remote sensing satellites. *Aerosol Air Qual Res* 20:1772–1782. <https://doi.org/10.4209/aaqr.2020.05.0240>
- Miller MR, Newby DE (2019) Air pollution and cardiovascular disease: car sick. *Cardiovas Res*. <https://doi.org/10.1093/cvr/cvz228>
- MITECO (2019) Ministry for ecological transition. environmental profile of Spain 2017. Indicator-based report. Page 18. https://www.miteco.gob.es/es/calidad-y-evaluacion-ambiental/publicaciones/pae2017_en_tcm30-487727.pdf. Accessed 26 Jan 2021
- Nakada LYK, Urban RC (2020) COVID-19 pandemic: Impacts on the air quality during the partial lockdown in São Paulo state. *Brazil Sci Total Environ* 730:139087. <https://doi.org/10.1016/j.scitotenv.2020.139087>
- Patel H, Talbot N, Salmond J, Dirks K, Xie S, Davy P (2020) Implications for air quality management of changes in air quality during lockdown in Auckland (New Zealand) in response to the 2020 SARS-CoV-2 epidemic. *Sci Total Environ* 746:141129. <https://doi.org/10.1016/j.scitotenv.2020.141129>
- Pei Z, Han G, Ma X, Su H, Gong W (2020) Response of major air pollutants to COVID-19 lockdowns in China. *Sci Total Environ* 743:140879. <https://doi.org/10.1016/j.scitotenv.2020.140879>
- Raffy G, Mercier F, Blanchard O, Derbez M, Dassonville C et al (2017) Semi-volatile organic compounds in the air and dust of 30 French schools: a pilot study. *Indoor Air* 27:114–127. <https://doi.org/10.1111/ina.12288>
- Rastogi YR, Sharma A, Nagraik R, Aygün A, Şen F (2020) The novel coronavirus 2019-nCoV: its evolution and transmission into humans causing global COVID-19 pandemic. *Int J Environ Sci Technol* 17:4381–4388. <https://doi.org/10.1007/s13762-020-02781-2>
- RD-ley 10/2020 (2020) de 29 de marzo, por el que se regula un permiso retribuido recuperable para las personas trabajadoras por cuenta ajena que no presten servicios esenciales, con el fin de



- reducir la movilidad de la población en el contexto de la lucha contra el COVID-19. <https://www.boe.es/boe/dias/2020/03/29/pdfs/BOE-A-2020-4166.pdf>. Accessed 2 Apr 2020
- RD 463/2020 (2020) de 14 de marzo, por el que se declara el estado de alarma para la gestión de la situación de crisis sanitaria ocasionada por el COVID-19. <https://www.boe.es/boe/dias/2020/03/14/pdfs/BOE-A-2020-3692.pdf>. Accessed 16 Mar 2020
- Rupani PF, Nilashi M, Abumalloh RA, Asadi S, Samad S, Wang S (2020) Coronavirus pandemic (COVID-19) and its natural environmental impacts. *Int J Environ Sci Technol* 17:4655–4666. <https://doi.org/10.1007/s13762-020-02910-x>
- Selvam S, Muthukumar P, Venkatramanan S, Roy PD, Bharath KM, Jesuraja K (2020) SARS-CoV-2 pandemic lockdown: effects on air quality in the industrialized Gujarat state of India. *Sci Total Environ* 737:140391. <https://doi.org/10.1016/j.scitotenv.2020.140391>
- Sharma S, Sharma P, Khare M, Kwatra S (2016) Statistical behavior of ozone in urban environment. *Sustain Environ Res* 26:142–148. <https://doi.org/10.1016/j.serj.2016.04.006>
- Sharma S, Zhang M, Anshika GJ, Zhang H, Kota SR (2020) Effect of restricted emissions during COVID-19 on air quality in India. *Sci Total Environ* 728:138878. <https://doi.org/10.1016/j.scitotenv.2020.138878>
- Suarez-Bertoa R, Zardini AA, Platt SM, Hellebust S, Pieber SM et al (2015) Primary emissions and secondary organic aerosol formation from the exhaust of a flex-fuel (ethanol) vehicle. *Atmos Environ* 117:200–211. <https://doi.org/10.1016/j.atmosenv.2015.07.006>
- Tello-Leal E, Macías-Hernández BA (2021) Association of environmental and meteorological factors on the spread of COVID-19 in Victoria, Mexico, and air quality during the lockdown. *Environ Res* 196:110442. <https://doi.org/10.1016/j.envres.2020.110442>
- WHOa (2020) Director-General's opening remarks at the media briefing on COVID-19, 11 March 2020. <https://www.who.int/dg/speeches/detail/who-director-general-s-opening-remarks-at-the-media-briefing-on-covid-19---11-march-2020>. Accessed 19 May 2020
- WHOb (2020) World Health Organization. Coronavirus disease 2019 (COVID-19): Situation report, 100. World Health Organization. <https://apps.who.int/iris/bitstream/handle/10665/332053/nCoVsitrep29Apr2020-eng.pdf?sequence=1&isAllowed=y>. Accessed 19 May 2020
- Xu Z, Nie W, Chi X, Huang X, Zheng L et al (2018) Ozone from fireworks: Chemical processes or measurement interference? *Sci Total Environ* 633:1007–1011. <https://doi.org/10.1016/j.scitotenv.2018.03.203>
- Yang Y, Sun L, Guo C (2018) Aero-material consumption prediction based on linear regression model. *Procedia Comput Sci* 131:825–831. <https://doi.org/10.1016/j.procs.2018.04.271>
- Yang Q, Yuan Q, Yue L, Li T (2020) Investigation of the spatially varying relationships of PM_{2.5} with meteorology, topography, and emissions over China in 2015 by using modified geographically weighted regression. *Environ Pollu* 262:114257. <https://doi.org/10.1016/j.envpol.2020.114257>
- Yuan Q, Qi B, Hu D, Wang J, Zhang J (2021) Spatiotemporal variations and reduction of air pollutants during the COVID-19 pandemic in a megacity of Yangtze River Delta in China. *Sci Total Environ* 751:141820. <https://doi.org/10.1016/j.scitotenv.2020.141820>
- Zalakeviciute R, Vasquez R, Bayas D, Buenano A, Mejia D et al (2020) Drastic improvements in air quality in Ecuador during the COVID-19 outbreak. *Aerosol Air Qual Res* 20:1783–1792. <https://doi.org/10.4209/aaqr.2020.05.0254>
- Zangari S, Hill DT, Charette AT, Mirowsky JE (2020) Air quality changes in New York City during the COVID-19 pandemic. *Sci Total Environ* 742:140496. <https://doi.org/10.1016/j.scitotenv.2020.140496>
- Zhang J, Cai Z, Yang B, Li H (2019) Association between outdoor air pollution and semen quality: protocol for an updated systematic review and meta-analysis. *Medicine* 98:e15730. <https://doi.org/10.1097/MD.00000000000015730>
- Zhao H, Ge Y, Tan J, Yin H, Guo J, Zhao W, Dai P (2011) Effects of different mixing ratios on emissions from passenger cars fueled with methanol/gasoline blends. *J Environ Sci* 23:1831–1838. [https://doi.org/10.1016/S1001-0742\(10\)60626-2](https://doi.org/10.1016/S1001-0742(10)60626-2)
- Zhou M, Huang Y, Li G (2021) Changes in the concentration of air pollutants before and after the COVID-19 blockade period and their correlation with vegetation coverage. *Environ Sci Pollu Res* 28:23405–23419. <https://doi.org/10.1007/s11356-020-12164-2>

Springer Nature or its licensor holds exclusive rights to this article under a publishing agreement with the author(s) or other rightsholder(s); author self-archiving of the accepted manuscript version of this article is solely governed by the terms of such publishing agreement and applicable law.

